ORIGINAL PAPER

Comparison of different digital elevation models for drainage morphometric parameters: a case study from South India

Venkatesh Kasi[1] · Ramdas Pinninti[1] · Sankar Rao Landa[1] · Maheswaran Rathinasamy[1] · Chandramouli Sangamreddi[1] · Rajeshwar Rao Kuppili[1] · Prasada Raju Dandu Radha[2]

Abstract

With a plethora of digital elevation models (DEM) available for elevation extraction and catchment morphometric analysis, it is essential to compare and investigate their accuracy and parameter uncertainty derived from them. To serve that purpose, in this study, we have compared the DEMs of different resolution obtained from Shuttle Radar Topography Mission (SRTM), CARTOSAT, and topographic maps (1:25000) in terms of vertical accuracy and morphometric parameters. The investigation was performed on a sub-basin of Champavathi River which is located in Andhra Pradesh, the southern part of India. The vertical accuracy of the DEMs was estimated using elevation from about 1180 points obtained from the Differential Global Positioning System (DGPS) survey. The morphometric analysis showed that the basin is elongated with low relief ratio, mild/rolling slopes, and medium drainage density, and the results were comparable from different DEM sources indicating that most of the morphometric parameters were not significantly dependent on the scale and source of the DEM. Further, vertical accuracy estimation showed that the CARTOSAT DEMs (10 m and 30 m) have a lower root mean square error (4.53 m and 5.89 m) when compared with the SRTM DEMs (6.11 m and 7.19 m).

Keywords Drainage morphometry · Comparison of DEM · Cartosat · Vertical accuracy

Introduction

With increasing urban population, the stress on existing water resources is multiplying manifolds. Further, with the uncertainties associated with the frequency and intensity of the rainfall, it becomes pertinent to evaluate the water resources availability as they play a significant role in the sustainable development of the economy. The excessive demand due to urban sprawl in countries like India puts stress in the available

ground and surface water supplies (Maheswaran et al. 2016; Sachindra et al. 2018), and it is essential to understand the present status of water resources before undertaking developmental projects.

The morphometric analysis is a critical component in evaluating the water resources and identifying the recharge sites, runoff modelling (Abdulkareem et al. 2018), soil erosion and flood susceptibility (Arabameri et al. 2020; Sarkar et al. 2020; Jothimani et al. 2020; Bajabaa et al. 2014), groundwater mapping, and watershed delineation (Thomas et al. 2012). Morphometric analysis results in useful information such as nature of the drainage pattern, topography, channel length, geological setup, nature of the rocks exposed, and slope of the terrain and quantitative description of drainage texture, pattern, and shape of the watershed. Strahler (1957), Smith (1950), and Horton (1945) provide the pioneering work in the area morphometry and form the basis of morphometric analysis and interpretation of their interrelationship concerning land and water management. With the advancement of technology, in terms of availability of satellite data and geographical information system (GIS) tools, the estimation of the morphometric parameters has become time-

✉ Maheswaran Rathinasamy
   maheswaran27@yahoo.co.in

1   Department of Civil Engineering, MVGR College of Engineering, Vizianagaram, Andhra Pradesh 535005, India

2   Department of Mechanical Engineering, MVGR College of Engineering, Vizianagaram, Andhra Pradesh 535005, India

efficient, accurate, and reliable (Jothimani et al. 2020; Niyazi et al. 2019; Banerjee et al. 2017; Grohmann et al. 2007; Hlaing et al. 2008; Javed et al. 2009). One of the critical inputs for the morphometric studies is the topographic elevation data. In this regard, digital elevation models (DEMs) have become essential data for not only morphometric analysis but also for hydrology and climatology studies (Jothimani et al. 2020; Setti et al. 2020; Kasi et al. 2020; Pankaj and Kumar 2009). DEMs have been frequently used for the morphometric analysis of river basins by extracting topographic parameters. DEM can be defined as a gridded representation of the spatial variation of the relief (Burrough et al. 2015).

The DEMs can be obtained from different sources, viz., topographic maps, field surveying using DGPS, radar interferometry, satellite data, drones, and contour maps. Out of these, satellite-based DEMs have gained popularity owing to the ease of availability and use. Some of the prominent satellite DEMs include SRTM (Farr et al. 2007), ASTER GDEM (Tachikawa et al. 2011), TanDEM-X (Gruber et al. 2012), ALOS AW3D DEM (Tadono et al. 2014), and CARTOSAT (Das et al. 2016; Patel et al. 2016). Several studies in the past have successfully used these DEMs for morphometric analysis of river basin all across the globe (e.g. Korup 2005; Lindsay and Evans 2008; Jacques et al. 2014; Caraballo-Arias et al. 2014; Masoud 2016; Rather et al. 2017; Jothimani et al. 2020; Abdeta et al. 2020). In the Indian context, some of the prominent studies which have used DEMs for morphometric analysis, river basin studies, and water resource evaluation include Setti et al. (2020); Sarkar et al. (2020); Ray et al. (2020); Agarwal et al. (2012); Aher et al. (2014); Banerjee et al. (2017); Das et al. (2016); Balasubramanian et al. (2017); Gopinath et al. (2018); Kannan et al. (2018); Satheeshkumar and Venkateswaran (2018); Prakash et al. (2019); Prabhakar et al. (2019); and Nitheshnirmal et al. (2019).

It is essential that the accuracy and precision of the results obtained from the morphometric analysis is a function of the spatial resolution of the DEM used, and it is generally accepted that the higher resolution DEMs are more precise and lead to accurate determination of the morphometric parameters (Das et al. 2016). Several studies have investigated the accuracy of individual DEMs and their effects on the extracted parameters such as drainage pattern, drainage area and length, and other morphometric parameters (Cook et al. 2012; Vaze et al. 2010; Weydahl et al. 2007). However, there are very few studies which have compared the accuracy of the different DEMS. For example, on the other hand, Rawat et al. (2019) compared the vertical accuracy of the SRTM, ASTER, and CARTOSAT (30 m) DEMs based on 20 ground control points. Mukherjee et al. (2013) evaluated open-source DEMs such as ASTER and SRTM using high postings CARTOSAT DEM and Survey of India (SOI) toposheet. Dikpal et al. (2017) used CARTOSAT(30 m) for

morphometric analysis of small watershed in Pinakini River Basin. Gopinath et al. (2015) compared the drainage network obtained using SRTM data with the ones obtained using the toposheet. Suwandana et al. (2012) compared the inundation area obtained using ASTER GDEM 2 with that of the GDEM1 and SRTM DEM. Other similar studies include Hosseinzadeh (2011) and Hirt et al. (2010). The studies, as mentioned above, were mainly directed towards the comparison of the absolute elevation parameters, and less focus was given to the various morphometric parameters. Within the knowledge of the authors, only a few studies have compared the morphometric analysis obtained using different DEMs and also for a specific region. For example, Das et al. (2016) have compared SRTM (30 m), ASTER (30 m), and CARTOSAT (30 m) in terms of the morphometric parameters derived using the corresponding DEMs for mountainous terrain. It is to be noted that there are few studies on comparing both vertical accuracy of the DEMs and the morphometric parameters from the DEMs. Further, there is no any study reported on the assessment of the fine resolution CARTOSAT DEM (10 m) in terms of morphometric analysis.

Therefore, the main aim of this study is to compare the morphometric properties derived from different DEMs sources and compare their vertical accuracy using the field-collected elevations. For this purpose, in this study, we have compared the morphometric properties of a small watershed draining to a lake in Andhra Pradesh, India, using freely and commercially available DEMs of different spatial resolution (CARTOSAT(10 m and 30 m) and SRTM (30 m and 90 m)) and topographic maps. This study compares morphometric properties, to name a few, like streams length, perimeter, basin length, basin relief, main channel fall, main channel length, relief ratio, basin relief/length, bifurcation ratio, drainage density, and main channel slope. Further, the vertical accuracy of the DEMs was estimated against the field-collected elevations at selected locations using DGPS survey.

Study area

In this study, we have considered a small watershed (shown in Fig. 1) which is draining through a lake/pond called Pedda Cherruvu (PC, hereafter). The study area is a sub-basin of the Champavathi River Basin in Southern India. The location of the watershed is between the latitude of 18° 11′ North and longitude of 83° 40′ East. The physiography of the watershed is dominated by plain areas with occasional small mountain ranges. The altitude ranges from 26 to 334 m. A substantial part of the study area is above 50-m elevation above the mean sea level. The major land cover and land use include agricultural tracts, urban area, hill slope, grasslands, and water bodies. The climate is characterized as high humidity almost throughout the year with extreme summer and adequate seasonal rainfall. The summer is generally
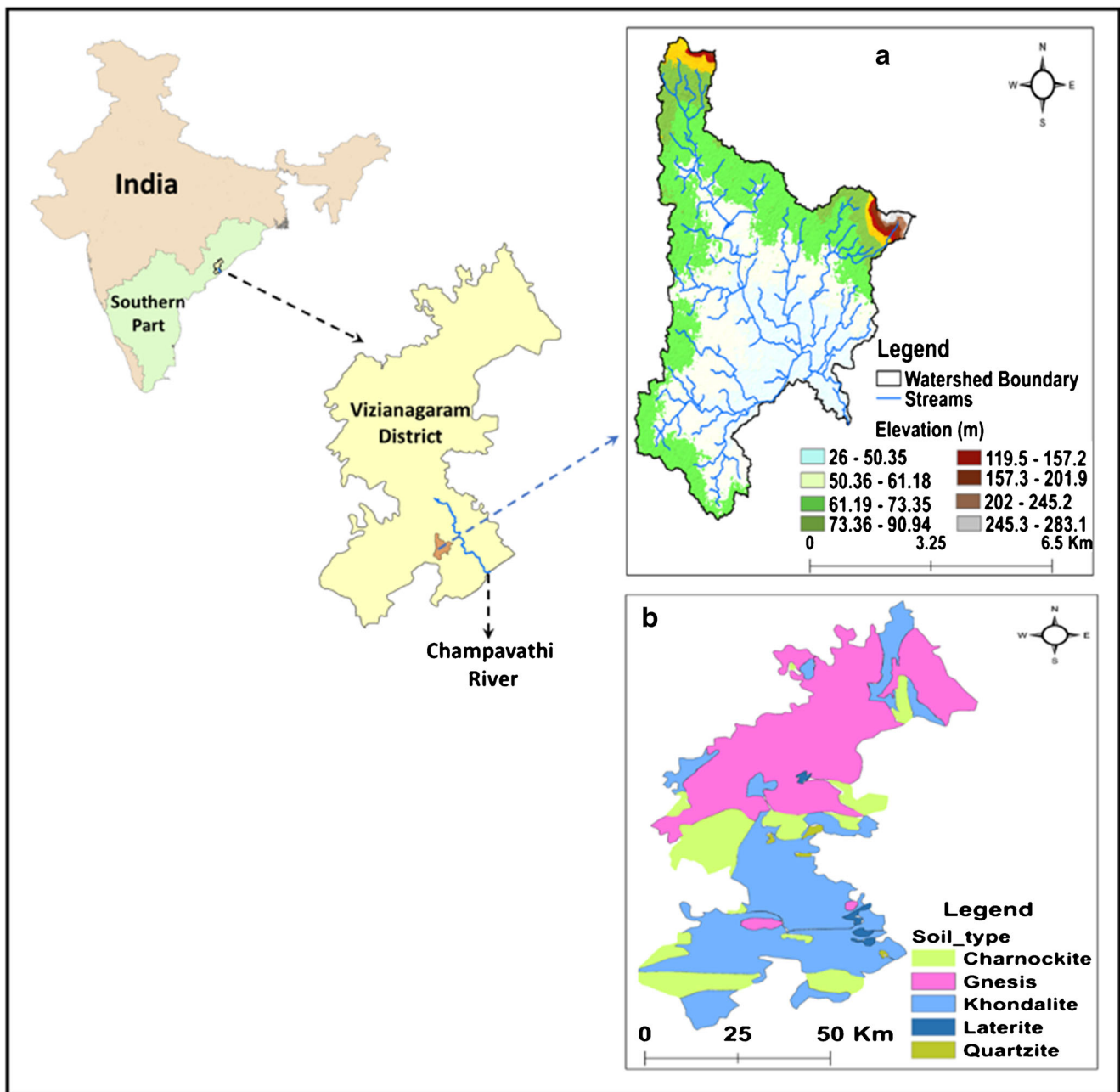
Fig. 1 (**a**) Index map showing the geographical location of the study area belongs to Southern part of India and also shows (**b**) lithology map of the study region (Source NRSC, India)

from March to June. The rainy season is followed in the form of South-West monsoon until the middle of October. Retreating monsoon is followed until November. The normal rainfall in this region is around 1100 mm.

From Fig. 1, it can be seen that the study area consists of consolidated formations which include crystallines (khondalites, charnockites, and granitic gneisses) and metasediments (the dolomites, shales, phyllites, and quartzites) of Archaean and Precambrian periods, respectively (NRSA 2007). The khondalite group of rocks can be seen as prominent hill ranges (strike ridges). Most parts of the study

area can be categorized as pediplain where the geomorphology features multi-concave, rock-cut erosion surface formed by the coalescence of two or more adjacent pediments and occasional desert domes, and representing the result of the mature stage of the erosion cycle.

Datasets and methods

The traditional approach for extracting the morphometric properties was based on manual calculation from the

topographic maps. However, such an approach has several limitations such as (i) the degree of drainage elaboration depends on the scale of the topographic map, (ii) errors may arise due to the disappearance of the channels as they reach the foothill zones (Das et al. 2016), and (iii) non-availability of the toposheet for certain parts due to security and defence reasons and many other as quoted by Das et al. (2016).

These limitations can be overcome by using the satellite-based DEM data; however, the accuracy and the reliability of these DEMs in representing the reality have to be estimated. The present study compares the DEMs derived from CARTOSAT-10 m DEM (commercially available), CARTOSAT-30 m, SRTM-30 m, and SRTM-90 m DEM and also evaluates the elevation accuracy using the DGPS data.

CARTOSAT-10 m and 30 m DEM

CARTOSAT is an 8Indian Satellite which was launched May 5, 2005, by Indian Space Research Organization (ISRO). CARTOSAT-1 satellite consists of a panchromatic camera which gives a long track of stereo, with a tilt in flight direction of ± 26° and ± 5°. CARTOSAT spacecraft gives the stereo images which can be used in different applications like large-scale mapping and terrain modelling (Kasi et al. 2020). It has coverage of 1 Arca Degree second, i.e. 30 m resolution. It can be freely downloaded from https://**bhuvan.nrsc.gov.in**. Further, CARTOSAT DEM of higher resolution (10 m) is made available and can be acquired from the National Remote Sensing Centre (NRSC), India. CARTOSAT-10 m resolution data has been used for this study area for comparison and was purchased from the National Remote Sensing Centre (NRSC).

Shuttle Radar Topography Mission (SRTM 30 m and 90 m)

The Shuttle Radar Topography Mission (SRTM) is an international project lead by the National Geospatial-Intelligence Agency and the National Aeronautics and Space Administration (NASA) (Zheng et al. 2015; Yue et al. 2017). It is a modified radar system which flew on an 11-day mission during February 2000 with onboard Space Shuttle Endeavour. The SRTM elevation data are derived from X-band, and C-band interferometric synthetic aperture radar (InSAR) sensor consists of a wavelength of 5.6 cm and frequency of 5.3 GHz. The SRTM digital elevation models (DEM) is obtained on a near-global scale from 56°S to 60°N (Farr and Kobrick 2000; Kasi et al. 2020). The SRTM DEM 30 m and 90 m datasets are freely available in https://earthexplorer.usgs.gov/ and can be downloaded based on scenes or tiles.

DGPS points

To calculate the accuracy of the DEMs, we have used the elevation data obtained from DGPS survey. For this purpose, we have considered around 1180 control points spread across the study area. The DGPS survey results were obtained from GEOCON Survey, Visakhapatnam, India. Kinematic GNSS approach using R95 receiver, which has a 95% confidence level. The vertical and horizontal accuracy of the equipment is 1.02 m and 0.6 m, respectively. The elevation from the DGPS locations was considered as an exact reference to estimate the error in DEMs.

SOI topsheet

The SOI topographical maps (Metric Edition, map sheet numbers 64 D/8 N) at 1:25,000 scale have been used for the preparation of the base map. These maps were prepared based on the surveys carried out in 1962–1963. In the selected study area, the streams were digitized manually, and in places where streams are not connected, they were connected based on the Google Earth images.

Datum correction

The publicly available DEM datasets like CARTOSAT, SRTM, and SOI toposheet have different horizontal and vertical datum, and the same has been presented in Table 1. Generally, the Differential Global Positioning System (DGPS) uses the vertical datum as WGS84 and takes the relative height as default (Mukherjee et al. 2013; Kaplan and Hegarty 2006). The derived DGPS elevation point is entirely different with obtained the earth surface elevation point, which is derived from mean sea level (MSL). The difference is due to variation among the WGS84 ellipsoid and geoid (local mean sea level). The geoid height is the constant geopotential surface or equipotential surface, which corresponds to mean sea level (MSL). The geoid height (or) geoid undulation (N) represents the difference between the geoid height and ellipsoid height at a particular point. Figure 2 compares the ellipsoid height (h) and orthometric height (H) which is measured above the geoid surface. Therefore, Eq. (1) represents how the ellipsoidal height (h) is computed using

Table 1 Horizontal and vertical datum of datasets used

S.No	Datasets	Horizontal datum	Vertical datum
1	Cartosat DEM	WGS84	WGS84
2	SRTM DEM	WGS84	ECM 96
3	DGPS	WGS84	WGS84
4	SOI toposheet	Everest	Mean sea level (MSL)

orthometric height (*H*) and geoid height (*N*):

$$h = H + N \tag{1}$$

Usually, the error present in the DEM datasets is estimated by taking the difference between the reference elevation data (Shortridge and Messina 2011). For comparison, DEM datasets like CARTOSAT, SOI toposheet, and DGPS elevation points were transferred from WGS84 to EGM96 geoid as a datum (Mukherjee et al. 2013; Kaplan and Hegarty 2006).

The geoid correction, i.e. orthometric heights to ellipsoidal height conversion, is done for CARTOSAT and DGPS data. The geoid correction conversion is done using ARC GIS tool. This tool applies the geoid model (EGM96) correction to the *z* values (elevation). For the conversion of vertical datum for different datasets, i.e. from orthometric heights to ellipsoidal heights using ARCGIS tool, the conversion process is available in https://desktop.arcgis.com/en/arcmap/10.3/manage-data/raster-and-images/wkflw- converting-from-orthometric-to-ellipsoidal-heights.htm.
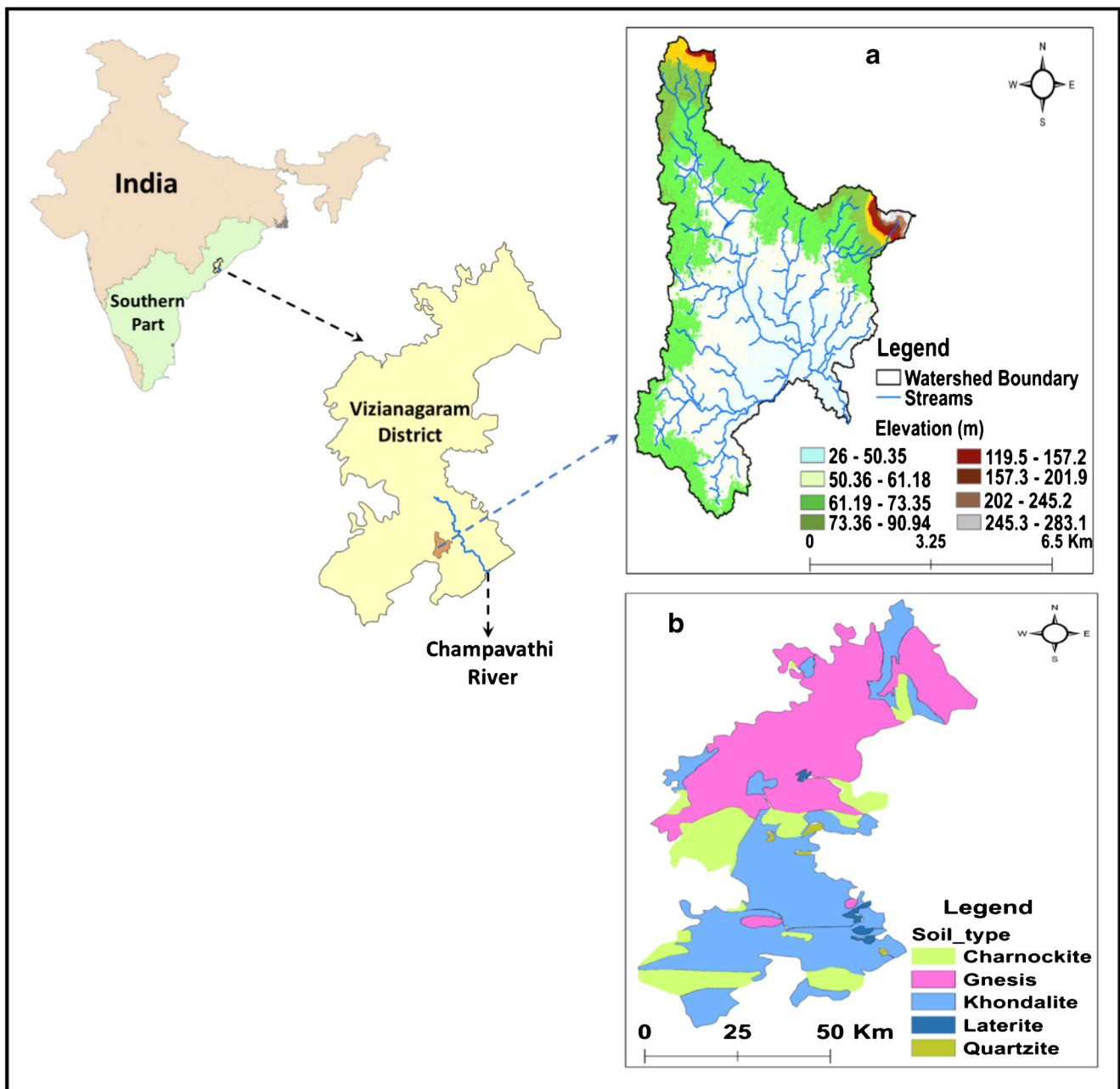

Fig. 2 Relation between ellipsoid height (*h*), orthometric height (*H*), and geoid undulation (*N*)

Table 2 Drainage morphometric parameters and their mathematical expression

S.No	Drainage morphometric parameters			Defined by	Derivation
	Measurements	Symbol	Dimensions		
1	Basin area	A	Km^2	Horton (1945)	--
2	Streams length	L_u	Km	Horton (1945)	--
3	Perimeter	P	Km	Smith (1950)	--
4	Basin length	L_b	Km	Schumm (1956)	--
5	Basin relief	H_b	m	Horton (1945) and Strahler (1964)	$Hb = Z_{max}\text{-}Z_{min}$
6	Main channel fall	H_c	m	---	--
7	Main channel length	C_m	Km	Strahler (1964) and Muller (1968)	--
8	No. of first-order streams	N_1	No	Strahler (1964)	--
9	No. of second-order streams	N_2	No	Strahler (1964)	--
Variables					
10	Relief ratio R = basin relief/length	R	m. Km^{-1}	Schumm (1956)	$R=\frac{Hb}{Lb}$
11	Drainage density	Dd	$Km. Km^{-2}$	Horton (1945)	$Dd=\frac{Lu}{A}$
12	Main channel slope	Sl	m. Km^{-1}	Horton (1945)	$Sl=\frac{Hc}{Cm}$
13	Elongation	Se	Dimensionless	Schumm (1956)	$Se = \frac{(A^{0.5}\times 2)}{(L\times\pi^{0.5})}$
14	Compactness constant	Sc	Dimensionless	---	$Sc=\frac{(P^2/A)}{(4\times\pi)}$
15	Length of overland flow	Lg	km	Horton (1945)	$Lg=\frac{1.0}{(2\times Dd)}$
16	Relative relief	Rm	Dimensionless	Melton (1957)	$Rm=\left(\frac{H_b}{P\times 1000}\right)$
17	Ruggedness number	Rg	Dimensionless	Strahler (1958)	$Rg=\left(\frac{H_b\times D_d}{1000}\right)$
18	Stream frequency	F	Km^{-2}	Horton (1945)	$F=\frac{(N1+N2-1)}{A}$
19	Drainage intensity	Di	Km^{-1}	---	$D_i=\left(\frac{F}{Dd}\right)$
20	Bifurcation ratio	R_b	Dimensionless	Horton (1945)	$B=\frac{N1}{N2}$
21	Drainage texture	D_t	Km^{-1}	(Horton, 1945)	$D_t = N_u/P$
22	Form factor	F_F	Dimensionless	Strahler (1952)	$F_F = A/L_b^2$
23	Shape factor	S_F	Dimensionless	(Miller 1953)	$S_F = L_b^2/A$
24	Circulatory factor	C_F	Dimensionless	Strahler (1964)	$C_F = (4*\pi*A)/P^2$

Methodology

Pre-processing of data

The pre-processing of the datasets was iteratively performed in terms of filling the data gaps, pit removal, and depression filling following the procedure outlined in Jenson and Domingue (1988). The derivation of DEMs from the SOI toposheet (1:25000) involved a time-consuming, laborious exercise which includes digitizing of the contour lines. Then, these were georeferenced using ground control points. The various contour lines thus obtained were used for generating the surface models with WGS84 as a datum.

Generation of stream networks and drainage area

Using the DEMs thus obtained from SOI toposheet and the satellite data, the stream network and drainage area of the study area were delineated using the following procedure.

We have used the eight-direction (D8) pour point model (Fairfield and Leymarie 1991) for calculating the flow direction for each pixel. Flow direction was calculated for each pixel using the filled DEM, i.e. the direction in which water would flow out of the pixel to one of the eight surrounding pixels. This concept is called the eight-direction (D8) pour point model (Fairfield and Leymarie 1991). Further, we have considered the Strahler (1954) method for ordering the streams, wherein each of the finger-tip tributaries was labelled are Order 1. When two streams of the same order meet, the order of resulting stream will increase by one.

The morphometric parameters were extracted from the datasets. The list of the parameter and the corresponding formulae and reference for estimating them is provided in Table 2. Most of the studies (Prabhakaran and Jawahar Raj 2018; Das et al. 2016; Banerjee et al. 2017; Mukherjee et al. 2013) used the parameters mentioned above for morphometric analysis. Further, other derived parameters which provide information about the linear, aerial, and relief aspects of

Fig. 3 Geograpical locations of the DGPS sample points used for estimating the vertical accuracy of the different DEM datasets
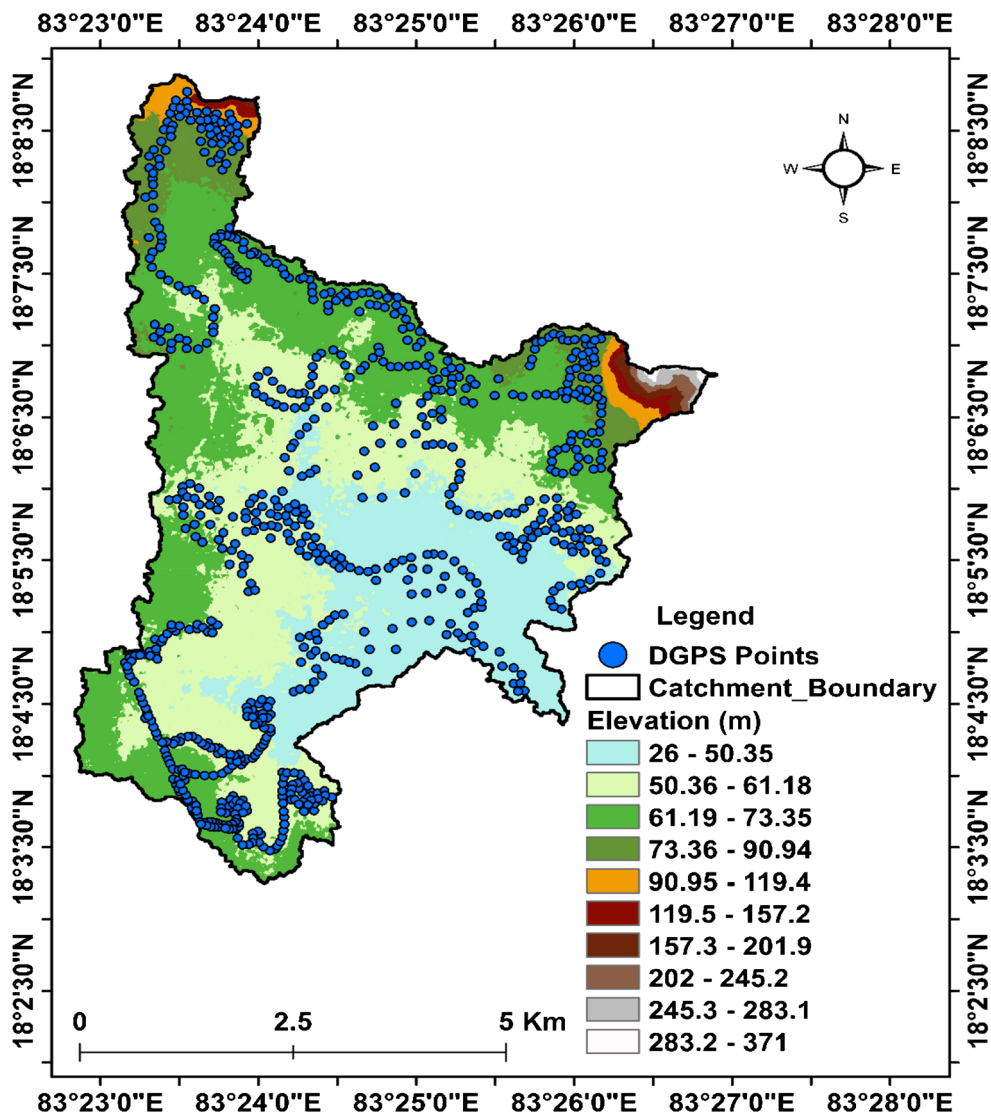
drainage are computed based on the formulas developed by Strahler (1952), Horton (1945), and Strahler (1964) as mentioned in Table 2. The definition and detailed discussion on the importance of each of these parameters can be found in the supplementary material.

Vertical error analysis

After the computation of the morphometric parameters, the vertical elevation error analysis was performed for the different DEMs with reference to DGPS points. We have considered the elevation of ground reference points obtained from the DGPS survey. The geographical spread and location of the DGPS points are shown in Fig. 3. It was also made sure that the DGPS survey points were collected in level areas within the basin and away from trees to reduce the errors due to signal tracking. Assuming that the values obtained from the DGPS survey is accurate of all the data sources. It is essential to mention that the data obtained

for different DEMs are converted to the same datum so that any error incurred due to difference in the datum is eliminated. Finally, the vertical accuracy comparison is estimated using DGPS control points, and other elevation values which are extracted from DEM generated from the CARTOSAT-10 m, CARTOSAT-30 m, and SRTM-30 m and SRTM-90 m.

The elevation points from the different DEMs were extracted using "point sampling tool" which is used as a plugin in QGIS. The accuracy of the DEMs was evaluated using the following measures: (i) root mean square error (RMSE) and (ii) mean absolute error (MAE):

$$\text{RMSE} = \sqrt{\frac{\sum_{i=1}^{N} \sum \left(Z_{\text{DEM}}^i - Z_{\text{DGPS}}^i \right)^2}{N}} \qquad (2)$$

$$\text{MAE} = \frac{\sum_{i=1}^{N} \sum \left| Z_{\text{DEM}}^i - Z_{\text{DGPS}}^i \right|}{N} \qquad (3)$$

Fig. 4 Error distribution from different DEMs in comparison with the DGPS points
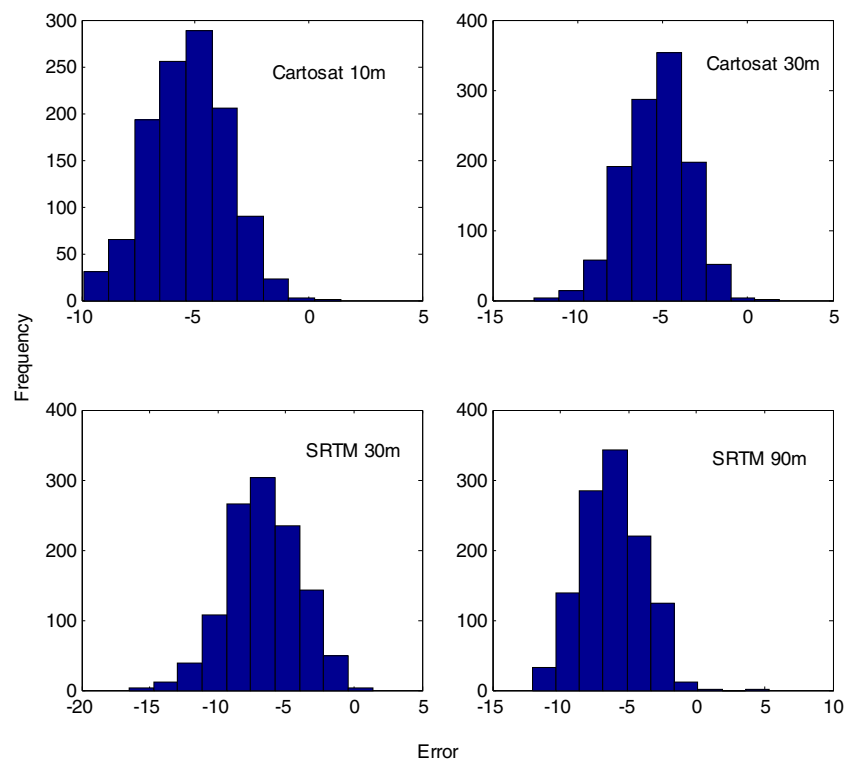
where $-Z_{DGPS}^{i}$ is elevation obtained using DGPS at ith sampling location, Z_{DEM}^{i} is the elevation obtained using DEM at i^{th} sampling location, and N is the total number of sampling points.

The performance evaluation metrics (RMSE and MAE) are based on the assumption that the errors follow a normal distribution. To test this, the frequency histograms are produced for each DEM, and the results show that the vertical errors follow the normal distribution (Fig. 4).

Results

Variation in morphometric parameters obtained from the different datasets

The quantitative drainage morphometric parameters were extracted from different DEMs. In the present study, the watershed for each of the case was delineated using the Arc Hydro Toolbox in ArcGIS-10 version. The watershed area and the stream networks are delineated and are found to be having dendritic drainage pattern, as shown in Fig. 5. According to Strahler (1954), dendritic drainage pattern shows homogeneity in texture, and there is no structural control. From each of the corresponding drainage network and the watershed area, the morphometric parameters were evaluated, and the same can be grouped as linear, relief, and areal parameters. In the following section, each set of parameters is discussed in detail, and their variation with respect to the DEM is used.

Linear parameters

The linear parameters, such as area, perimeter, stream order, number of streams for each order, bifurcation ratio, and length of streams, have been estimated and reported in Table 3. It was found that there is a small variation in the basin areas extracted from different DEMs, but there were significant changes in the basin shape measured in terms of the perimeter. Figure 6 shows the superposition of the catchment boundary as obtained from different datasets. The basin length was found to be similar for all the datasets used in this study. Analysis of the basin elevation in terms of minimum and maximum shows that there is a difference in the on the order of 6–14 m between the CARTOSAT 10 m and other DEMs.

Stream order (N) It is observed that CARTOSAT 30 m and SRTM 90 m generate the maximum numbers of streams. Moreover, the highest order of 4 (obtained using the scheme given by Strahler 1954) is depicted by all the datasets. The log of the number of streams for each order is plotted (see Fig. 7) against the stream order, and it reveals an inverse geometric sequence. In practice, when logarithms of the number of streams of a given order are plotted against the order, the points lie on a straight line (Horton 1945). The streams obtained using all the DEMs showed linear relationship, whereas the fine resolution CARTOSAT 10 m is close to the one obtained using the toposheet 1:25000. Overall, from the pattern of relationship between the number of streams in a given order and order number, it can be said that the whole area has
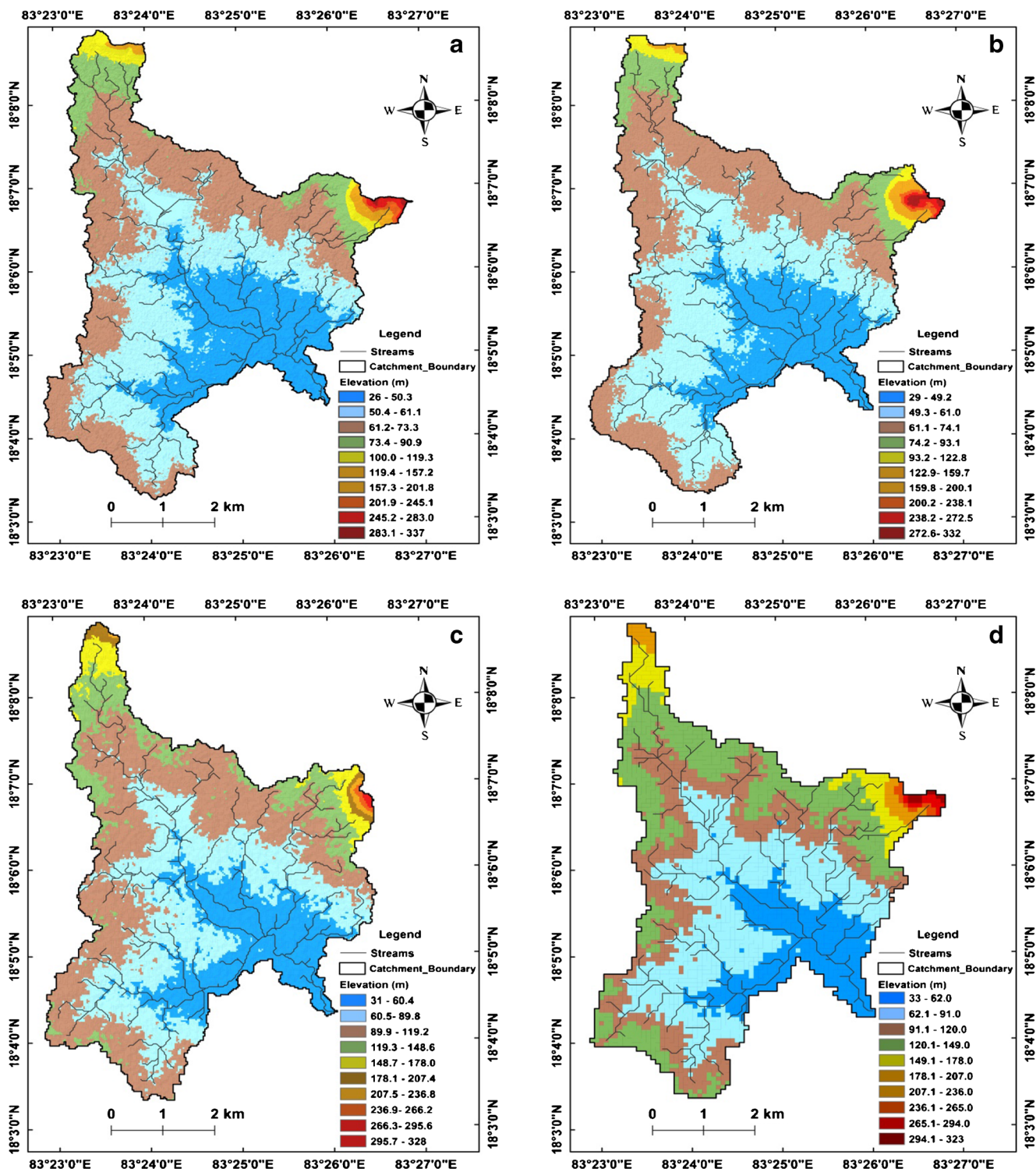
Fig. 5 Maps showing the catchment boundary, draining pattern obtained using (**a**) Cartosat 10 m, (**b**) Cartosat 30 m, (**c**) SRTM 30 m, and (**d**) SRTM 90 m

uniform lithology, and there has been no probable uplift in the study area.

**Stream length (*Lu*)** In the case of stream lengths, it is observed that the overall stream lengths were highest for the CARTOSAT 10 m and 30 m. On the other hand, there is a decrease in length obtained from the SRTM DEMs. Further, the DEMs obtained from the topographical maps result in a lower number of streams as the numbers of contour lines were minimal in the study area.

Table 3   The morphometric properties of the Pedda Cherruvu watershed derived from the different datasets

S.No	Drainage morphometric parameters			Cartosat 10 m	Cartosat 30 m	SRTM 30 m	SRTM 90 m	SOI toposheet 1:25000
	Measurements	Symbol	Units					
1	Basin area	A	Km^2	33.73	32.78	33.15	32.15	34
2	Streams length	Lu	km	91.27	86.89	82.43	82.50	81.69
3	Perimeter	P	km	56.34	50.44	48.74	43.83	55
4	Basin length	L_b	km	9.02	9.02	9.02	9.02	9
5	Basin relief	H_b	m	311	303	297	290	272
6	Main channel fall	Hc	m	11	8	9	11	13
7	Main channel length	Cm	Km	3.02	2.83	2.92	2.75	2.72
8	No. of first-order streams	$N1$	No	74	85	75	87	105
9	No. of second-order streams	$N2$	No	13	14	15	15	51
Variables								
10	Relief ratio R = basin relief/length	R	$m.Km^{-1}$	0.034	0.034	0.033	0.032	0.0322
11	Drainage density	Dd	$Km. Km^{-2}$	2.70	2.65	2.48	2.55	2.69
12	Main channel slope	SL	$m.Km^{-1}$	3.63	2.82	2.87	2.26	4.79
13	Elongation ratio	Se	Dimensionless	0.72	0.71	0.72	0.70	0.73
14	Compactness constant	Sc	Dimensionless	2.74	2.00	2.38	2.18	2.66
15	Length of overland flow	Lg	km	0.184	0.188	0.201	0.195	0.18
16	Relative relief	Rm	Dimensionless	0.0055	0.006	0.0061	0.0066	0.0054
17	Ruggedness number	Rg	Dimensionless	0.83	0.80	0.68	0.741	0.73
18	Stream frequency	F	Km^{-2}	2.58	3.02	2.72	3.17	2.6
19	Drainage intensity	Di	Km^{-1}	1.610	1.945	1.807	2.103	2.29
20	Bifurcation ratio	R_b	Dimensionless	5.69	6.07	5	5.8	4.05
21	Drainage texture	D_t	Km^{-1}	1.54	1.96	1.85	2.33	4.94
22	Form factor	F_F	Dimensionless	0.42	0.40	0.41	0.39	0.4
23	Shape factor	S_F	Dimensionless	2.41	2.48	2.45	2.53	2.38
24	Circulatory factor	C_F	Dimensionless	0.13	0.16	0.17	0.21	0.135

Fig. 6 Catchment boundray delineated using different sources of DEM
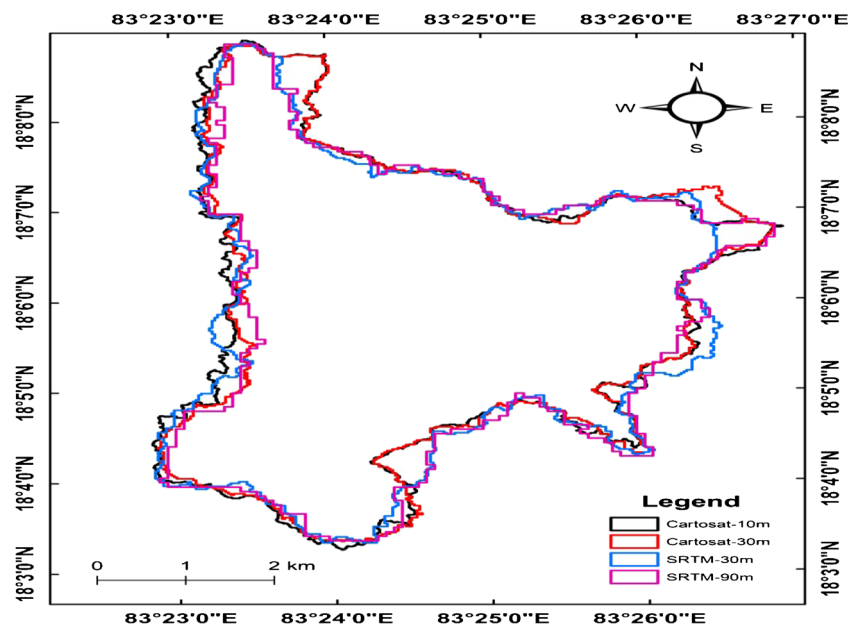
Fig. 7 Graph between logarithm of number of streams in given order vs stream order obtained using different datasets
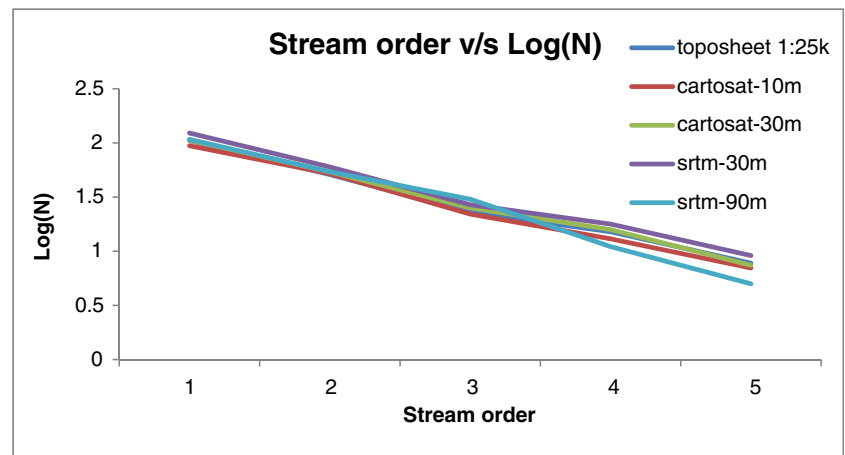
Bifurcation ratio (Rb) Bifurcation ratio is a function of geological structure and permeability of the surface strata (Strahler 1964; Esper Angillieri 2008; Giusti and Schneider 1965; Chow 1964), and according to the Horton (1945), it can be considered as an index of relief. For basins, with no disturbance from geologic structures, the general range of bifurcation ratios is between 3.0 and 5.0 (Strahler 1964). Mesa (2006) suggests that for basins with R_b, more than 10, show the influence of geological structures on the drainage pattern.

Analysis of hydrographs and evaluation of surface water potential of a watershed can be done using the bifurcation ratio (Esper Angillieri 2008; Jain et al. 2000).

From Table 3, the bifurcation ratio for the first two orders of streams obtained from all DEMs and SOI toposheet has values between 4 and 6, indicating that the streams formed inhomogeneous rock with minimal or no influence of geological structures. The bifurcation values imply that for every second-order stream, there are approximately 4–6 first-order streams.

Relief parameters

Basin relief (H_b) This parameter plays a significant role in drainage development, surface and sub-surface water flow, permeability, landform development, and erosion properties of the terrain (Obi Reddy et al. 2004). Further relief measures are essential in understanding the denudational characteristics of the landforms and the watershed (Farhan 2017). Generally, higher basin relief (H_b) value indicates that gravity flow would dominate, resulting in low infiltration and high runoff in the basin (Ozdemir and Bird 2009). For the study area, basin relief (H_b) values obtained from the different data vary from 272 (using SOI toposheet) to 311(CARTOSAT 10 m), and the values from the different DEMs do not vary significantly from each other. Overall, the results show that the basin relief value of the study area is moderate, indicating that the basin generates low runoff and has more infiltration (Strahler 1954).

Relief ratio (R_h) It is the ratio of the basin relief to the longest basin length parallel to the principal stream (Schumm 1954). It provides an estimate of the overall steepness of the basin (Schumm 1956), and it is a measure of the intensity of erosion process (Ajibade et al. 2010) and also an indicator of available potential energy for driving water and sediment movement (Sarkar and Gundekar 2007). The relief ratios obtained from the DEMs are in the close range, and it can be said that the basin has low relief ratio on the order of 0.03. The value of relief ratio from all the DEMs was found to be having comparable values around 0.032, indicating that the presence of gentle/rolling slopes in the catchment leading for the lower intensity of erosion process in the basin.

Ruggedness number (R_n) Ruggedness number (R_n) is a non-dimensional parameter. It is a product of drainage density and relative relief. R_n captures slope steepness and length and represents the structural complexity of the terrain (Strahler 1957). High values of R_n would occur when both variables, relative relief and drainage density, are large, and for such basins, the slopes are not only steep but are also long. Basins with high R_n values are highly susceptible to erosion and, therefore, susceptible to an increased peak discharge.

On the other hand, lower values indicate mild slope and moderate length leading to a lesser chance of erosion. For the study area, CARTOSAT DEM shows that the basin is having a value of ruggedness number around 0.8, whereas the SRTM DEM-based analysis shows the value varies between 0.68 and 0.74. From these values and referring to Altaf et al. (2013) and Prabhakaran and Jawahar Raj (2018), the ruggedness number is low, and therefore, the basin is not susceptible to erosion.

Areal parameters

Elongation ratio (R_e) It is defined as the ratio between the diameter of the circle of the same area of a circle having area as that of the watershed and maximum length of the catchment (Schumm 1956). Generally, the values of Re vary between 0.6

and 1.0 depending on the geology and climate of the catchment. The values can be categorized into three groups, namely, (i) circular (> 0.9), (ii) oval (0.9 to 0.7), and (iii) elongated (< 0.7). Higher values R_e close to unity are associated with low relief, whereas values in the range of 0.6–0.8 are usually connected with high relief and steep ground slope (Strahler 1964). Also, higher values of R_e (> 0.7) indicate low relief and high infiltration, and low runoff and lower values of R_e indicate high erosion and lesser infiltration rates (Strahler 1954; Obi Reddy et al. 2004; Rai et al. 2017).

For the study region, the elongation ratio was found to be varying from 0.72 to 0.73 from the different DEMs, indicating that the basin is oval shape and possesses flat slope, more infiltration, and lower runoff.

Stream frequency (F_s) Stream frequency, according to Horton (1945), is the total number of streams of all orders per unit area of the catchment. In the study area, the stream frequencies obtained from all DEMs are in a similar range varying from 2.58 to 3.17 streams per sq. Km. Stream frequency is directly related to runoff (Pankaj and Kumar 2009) and degree of dissection and inversely related to infiltration and mean annual rainfall (Morisawa 1962). Comparing the results from the other studies such as Das et al. (2016) and Prabhakaran and Jawahar Raj (2018), the value of F_s for the present study region can be considered low, thereby implying a general tendency to have more infiltration and less runoff.

Drainage density (D_d) The drainage density is computed as the ratio of the length of the streams and area of the watershed (Horton 1932). Drainage density is having direct relationship with rock resistivity (Sangireddy et al. 2016), mean annual rainfall (Morisawa 1962), rainfall intensity, and an inverse relationship with infiltration capacity (Horton 1945), permeability (Strahler 1956) and vegetation cover (Prabhakaran and Jawahar Raj 2018). The lower values of D_d results in the areas have permeable subsoil material or highly resistant, low relief and have dense vegetation (S K Nag 1998). Higher values of D_d correspond to catchment having a more significant number of streams and thus result in rapid stream response, whereas low drainage density implies lower runoff and higher infiltration (Chorley 1969).

Strahler (1957) classified the basins into different categories based on D_d values: (i) course (< 5 km^{-1}), (ii) medium (5.00 to 13.7 km^{-1}), (iii) fine (13.7 to 155.3 km^{-1}), and (iv) ultra-fine (> 155 km^{-1}).

From the results obtained for the study area, the D_d values from different DEMs vary from 2.48 to 2.70 km^{-1} correspond to coarse drainage density indicating lower runoff and more infiltration characteristics, permeable subsurface material and has dense vegetation (Agarwal et al. 2012; Chopra et al. 2005). These characteristics suggest that the study area is highly suitable for groundwater recharge.

Length of overland flow (Lg) Horton (1945) defines the length of overland flow as half the reciprocal of drainage density, and it describes the length of the water flow over the surface before it joins the streams. For the present study, the values of Lg vary from 0.18 to 0.20 km, and variation among the different dataset is minimal. Generally, in a catchment with smaller Lg values (< 0.01 km), the overland flow runoff would enter the stream faster, and even small amount of rainfall can contribute to a significant quantity of the streamflow. Olszevski et al. (2011) suggest that lower values of Lg indicate flooding situation in the catchment during days of heavy rainfall due to less contact with the soil surface and thereby low infiltration. Based on the above inferences, for the study region, the length of overland flow is moderate; thereby, rainfall would enter the streams slowly with lag time and less prone to the flooding situation.

Drainage texture (T) It is defined as the ratio of a total number of streams of all orders to the perimeter of that area (Horton 1945). According to Horton (1945), infiltration capacity can be recognized as the single critical factor which influences drainage texture and considered drainage texture to comprise both drainage density and stream frequency. However, Smith (1950) showed that drainage texture depends on several physical factors such as rainfall, climate, soil type, vegetation, relief, infiltration capacity, and stage of development of the basin. Based on the drainage texture values, Smith (1950) classified it into the five different groups, very fine (> 8), fine (6–8), moderate (4–6), coarse (2–4), and very coarse (< 2). Coarser drainage texture implies the watershed has larger basin lag periods than the fine-textured basins. From the values for drainage texture reported in Table 3, the DEM-based analysis shows that the study region is very coarse, whereas the SOI toposheet-based results indicate that it moderate.

The form factor (F_F) The ratio of the area of the basin to the square of the basin length is defined as the form factor (Horton 1945). The form factor is one of the critical parameters which represents the shape of the catchment area. The form factor value 0.7854 would be indicative of the circular catchments, and hence, form factor value should be less or equal to the circular catchments value (Chopra et al. 2005). Higher form factor leads to a peak flow of the shorter duration, whereas the basins with lower form factor have an elongated shape, and lower peaks flow for longer durations. For the present case study, the form factor values vary in between 0.39 (SRTM 90 m) and 0.42 (CARTOSAT-10 m) and represent the catchment shape as elongated shape and having the lower peak flow for the longer duration.

Shape factor (S_F) The shape factor is inverse of the form factor and is defined as the ratio of the square of the basin length to the area of the basin (Horton 1945). The measured shape factor does not show much variation (least 2.41 CARTOSAT 10 m and

Table 4 Assessment of vertical accuracy of Different DEMs using the DGPS survey

S.NO	Statistic	CARTOSAT-10 M	CARTOSAT-30 M	SRTM-30 M	SRTM-90 M
1	Mean elevation (m)	34.08	34.10	34.86	35.21
2	Variance of elevation (m)	69.03	68.89	79.87	85.96
3	Root mean square error (m)	4.53	5.89	6.11	7.19
4	Mean absolute error (m)	4.39	5.40	6.22	6.64

highest 2.53 SRTM 90 m) for the present study area from the different source and values from all sources indicates that the basin flat and having the low peak flow for the longer duration.

Circulatory factor (C_F) The circulatory factor is the ratio of the basin area to the area of the circle having the circumference as the perimeter as a basin (Miller 1953). The parameters like length, land use/land cover, climate, relief, frequency of the streams, and geological structure of the basin will influence the circulatory factor. The higher the circulatory factor indicates that the catchment is circular and will indicate higher peaks to the shorter duration and vice versa. In the present study, circulatory factor values are calculated for the same basin by using the four different sources of the available data (mentioned in Table 3). The highest value is 0.21 for the SRTM 90 m, and lowest is being 0.13 for the CARTOSAT 10 m. The values from all the sources of the data indicate that the catchment is flatter, and lower peaks will be obtained for a longer duration.

Vertical error

From the above analysis, it was observed that the morphometric attributes of the basin are least sensitive to the type and resolution of the dataset from which they were derived. We have compared the obtained DGPS elevation points with the ones obtained from DEMs. Using the difference in elevations, the vertical error analysis was performed for all the DEMs. The RMSE and the MAE were calculated using 200 points, and the results statistics are tabulated in Table 4. The analysis of the results in terms of RMSE shows that the CARTOSAT 10 m DEM show less deviation from the DGPS data, whereas the SRTM DEMs show higher level of error. The RMSE of the CARTOSAT 10 m data is around 5 m which is considerably less when compared with the SRTM DEMs. It is noted that these observations are contradictory to the ones obtained by Das et al. (2016), where it was observed that for mountainous region, SRTM performed better than the CARTOSAT 30 m DEM.

Therefore, it can be inferred with a reasonable degree of confidence that CARTOSAT DEMs are reliable options for morphometric analysis, particularly in regions where topographic maps are not available at fine resolution.

Discussion

Overall, the present study compared different DEMs in terms of vertical accuracy and morphometric analysis. The present study is unique owing to the availability of DGPS data which were used to estimate the vertical accuracy of different DEMs.

From the results of the morphometric analysis in terms of different parameters, it was observed that for most of the parameters, the values from the different DEMs were not varying much and were within the comparable range of SOI toposheet-based estimates. This indicates that the DEMs can be reliably used in the study area for conducting morphometric studies. Each of these parameters has a certain implication on hydrology and water resources management in the study region. Drainage morphometric analysis of the watershed reveals information about the evolution of land surface process and its formation and also the hydrologic behaviour of watershed (Rahmati et al. 2019; Aouragh and Essahlaoui 2018; Arabameri et al. 2018).

For the watershed considered in the study, it was observed that there is no significant influence of geological structures on drainage development. The area is well drained by streams of order up to 4 showing moderate runoff generation from the watershed. Likewise, from the stream length results, there is no likely uplift in the basin because the watershed area depends only on the drainage characteristics for movement of water. Therefore, the longer movement of water makes the watershed hydrologically very active (Luo and Harlin 2003). The geometric relationship between the stream order and the stream number implies that the watershed has uniform underlying lithology, and it is geologically stable. Likewise, stream length values suggest that there is no likely uplift in the basin because the watershed area depends only on the drainage characteristics for the movement of water. The stream frequency values imply that the watershed has adequate infiltration capacity and a fair amount of vegetation. Due to high infiltration capacity in the watershed, the discharge takes a longer time to peak. The bifurcation ratio 5–6, concerning

the hydrology and water resources, in the study area, is highly welcome as it is favourable for watershed development activities, particularly in the semi-arid regions of the Vizianagaram district. The drainage texture and the form factor showed that the basin is having moderate to coarse drainage and is elongated in shape characterized by low peak discharges. Lower values of drainage density in the study area imply low surface runoff and high infiltration and therefore comparably are good sites for water harvesting structures (Dodov and Foufoula-Georgiou 2005; Chopra et al. 2005; Luo and Harlin 2003). From the different morphological parameters investigated in this study, it is concluded that the study region is permeable and is suitable for groundwater recharging and water harvesting structures. This information can help in watershed management practices and flood management.

Conclusion

Morphometric analysis plays a vital role in many applications related to water resources management and flood control. With the advancement of technology, the digital elevation models have been increasingly used in geomorphological studies and have, to a greater extent, replaced the traditional methods based on topographic maps. This is mainly because of the ease in obtainability, using and extracting the parameters. However, with the availability of different sources of DEMs, it becomes pertinent to choose the right one for the analysis. With this motivation, the present study was aimed towards comparing the different commonly used DEMs and identifies the best for computing the morphometric parameters for a plain area. From the analysis of the results obtained from the different DEMs, it is observed that the CARTOSAT 10 m and 30 m are more accurate in comparison with the SRTM DEMs in terms of vertical elevation. However, based on the morphometric analysis, the parameters estimated were not highly sensitive to the data sources (used in this study) and therefore resulted in similar results. It is also observed that the comparison between CARTOSAT 10 m and 30 m showed comparable results, and thus, these DEMs can be reliably used for drainage delineation where toposheet is not available.

Based on the morphometric analysis of the study region, it is concluded that this region in Champavathi River Basin is mild sloped, with vegetation cover and high infiltration capacity and low runoff, and therefore, it is having good groundwater prospect and suitable for water harvesting structures.

References

Abdeta GC, Tesemma AB, Tura AL, Atlabachew GH (2020) Morphometric analysis for prioritizing sub-watersheds and management planning and practices in Gidabo Basin, Southern Rift Valley of Ethiopia. Appl Water Sci 10:1–15

Abdulkareem JH, Pradhan B, Sulaiman WNA, Jamil NR (2018) Quantification of runoff as influenced by morphometric characteristics in a rural complex catchment. Earth Syst Environ 2:145–162

Agarwal KK, Prakash C, Ali SN, Jahan N (2012) Morphometric analysis of the Ladhiya and Lohawati river basins, Kumaun Lesser Himalaya, India. Z Geomorphol 56:201–224

Aher PD, Adinarayana J, Gorantiwar SD (2014) Quantification of morphometric characterization and prioritization for management planning in semi-arid tropics of India: a remote sensing and GIS approach. J Hydrol 511:850–860. https://doi.org/10.1016/j.jhydrol.2014.02.028

Ajibade L, Ifabiyi L, Iroye K, Ogunteru S (2010) Morphometric analysis of Ogunpa and Ogbere drainage basins, Ibadan, Nigeria. Ethiop J Environ Stud Manag 3:1–19. https://doi.org/10.4314/ejesm.v3i1.54392

Altaf F, Meraj G, Romshoo SA (2013) Morphometric analysis to infer hydrological behaviour of Lidder watershed, Western Himalaya, India. Geogr J 2013:1–14. https://doi.org/10.1155/2013/178021

Aouragh MH, Essahlaoui A (2018) A TOPSIS approach-based morphometric analysis for sub-watersheds prioritization of high Oum Er-Rbia basin, Morocco. Spat Inf Res 26:187–202. https://doi.org/10.1007/s41324-018-0169-z

Arabameri A, Pradhan B, Pourghasemi HR, Rezaei K (2018) Identification of erosion-prone areas using different multi-criteria decision-making techniques and gis. Geomatics Nat Hazards Risk 9:1129–1155. https://doi.org/10.1080/19475705.2018.1513084

Arabameri A, Tiefenbacher JP, Blaschke T, Pradhan B, Bui DT (2020) Morphometric analysis for soil erosion susceptibility mapping using novel gis-based ensemble model. Remote Sens 12:1–24. https://doi.org/10.3390/rs12050874

Bajabaa S, Masoud M, Al-Amri N (2014) Flash flood hazard mapping based on quantitative hydrology, geomorphology and GIS techniques (case study of Wadi Al Lith, Saudi Arabia). Arab J Geosci 7(6):2469–2481. https://doi.org/10.1007/s12517-013-0941-2

Balasubramanian A, Duraisamy K, Thirumalaisamy S, Krishnaraj S, Yatheendradasan RK (2017) Prioritization of subwatersheds based on quantitative morphometric analysis in lower Bhavani basin, Tamil Nadu, India using DEM and GIS techniques. Arab J Geosci 10:1–18. https://doi.org/10.1007/s12517-017-3312-6

Banerjee A, Singh P, Pratap K (2017) Morphometric evaluation of Swarnrekha watershed, Madhya Pradesh, India: an integrated GIS-based approach. Appl Water Sci 7:1807–1815. https://doi.org/10.1007/s13201-015-0354-3

Burrough PA, McDonnell R, McDonnell RA, Lloyd CD (2015) Principles of geographical information systems. Oxford university press

Caraballo-Arias NA, Conoscenti C, Di Stefano C, Ferro V (2014) Testing GIS-morphometric analysis of some Sicilian badlands. Catena 113:370–376. https://doi.org/10.1016/j.catena.2013.08.021

Chopra R, Dhiman RD, Sharma PK (2005) Morphometric analysis of sub-watersheds in Gurdaspur district, Punjab using remote sensing and GIS techniques. J Indian Soc Remote Sens 33:531–539. https://doi.org/10.1007/BF02990738

Chorley RJ (1969) Water, earth, and man. A synthesis of hydrology, geomorphology, and socio-economic geography. Water, earth, and man. A synthesis of hydrology, geomorphology, and socio-economic geography

Chow VT (1964) Handbook of applied hydrology

Cook AJ, Murray T, Luckman A, Vaughan DG (2012) A new 100-m digital elevation model of the antarctic peninsula derived from

ASTER Global DEM: methods and accuracy assessment. Earth Syst Sci Data 4:129–142. https://doi.org/10.5194/essd-4-129-2012

Das S, Patel PP, Sengupta S (2016) Evaluation of different digital elevation models for analyzing drainage morphometric parameters in a mountainous terrain: a case study of the Supin–Upper Tons Basin, Indian Himalayas. Springerplus 5:1–38. https://doi.org/10.1186/s40064-016-3207-0

Dikpal RL, Renuka Prasad TJ, Satish K (2017) Evaluation of morphometric parameters derived from Cartosat-1 DEM using remote sensing and GIS techniques for Budigere Amanikere watershed, Dakshina Pinakini Basin, Karnataka, India. Appl Water Sci 7:4399–4414. https://doi.org/10.1007/s13201-017-0585-6

Dodov B, Foufoula-Georgiou E (2005) Fluvial processes and streamflow variability: Interplay in the scale-frequency continuum and implications for scaling. Water Resour Res 41:1–18. https://doi.org/10.1029/2004WR003408

Esper Angillieri MY (2008) Morphometric analysis of Colangüil river basin and flash flood hazard, San Juan, Argentina. Environ Geol 55:107–111. https://doi.org/10.1007/s00254-007-0969-2

Fairfield J, Leymarie P (1991) Drainage networks from grid digital elevation models. Water Resour Res 27(5):709–717. https://doi.org/10.1029/90WR02658

Farhan Y (2017) Morphometric assessment of Wadi Wala watershed, Southern Jordan Using ASTER (DEM) and GIS. J Geogr Inf Syst 09:158–190. https://doi.org/10.4236/jgis.2017.92011

Farr TG, Kobrick M (2000) Shuttle radar topography mission produces a wealth of data. EOS Trans Am Geophys Union 81:583. https://doi.org/10.1029/EO081i048p00583

Farr TG, Rosen PA, Caro E, Crippen R, Duren R, Hensley S, Kobrick M, Paller M, Rodriguez E, Roth L, Seal D (2007) The Shuttle Radar Topography Mission. Rev Geophys 45:2

Giusti EV, Schneider WJ (1965) The distribution of branches in river networks. US Government Printing Office

Gopinath G, Ambili GK, Gregory SJ, Anusha CK (2015) Drought risk mapping of south-western state in the Indian peninsula - a web based application. J Environ Manag 161:453–459. https://doi.org/10.1016/j.jenvman.2014.12.040

Gopinath G, Ramisha N, Nair AG, Jesiya NP (2018) Spatial characters of a tropical river basin, south-west coast of India. In Hydrologic modeling (pp. 641–657). Springer, Singapore. https://doi.org/10.1007/978-981-10-5801-1_44

Grohmann CH, Riccomini C, Alves FM (2007) SRTM-based morphotectonic analysis of the Poços de Caldas Alkaline Massif, southeastern Brazil. Comput Geosci 33:10–19. https://doi.org/10.1016/j.cageo.2006.05.002

Gruber A, Wessel B, Huber M, Roth A (2012) Operational TanDEM-X DEM calibration and first validation results. ISPRS J Photogramm Remote Sens 73:39–49. https://doi.org/10.1016/j.isprsjprs.2012.06.002

Hirt C, Filmer MS, Featherstone WE (2010) Comparison and validation of the recent freely available ASTER-GDEM ver1, SRTM ver4.1 and GEODATA DEM-9 s ver3 digital elevation models over Australia. Aust J Earth Sci 57:337–347. https://doi.org/10.1080/08120091003677553

Hlaing KT, Haruyama S, Aye MM (2008) Using GIS-based distributed soil loss modeling and morphometric nalysis to prioritize watershed for soil conservation in Bago river basin of Lower Myanmar. Front Earth Sci China 2:465–478. https://doi.org/10.1007/s11707-008-0048-3

Horton RE (1932) Drainage-basin characteristics. EOS Trans Am Geophys Union 13:350–361. https://doi.org/10.1029/TR013i001p00350

Horton RE (1945) Erosional development of streams and their drainage density: hydrophysical approach to quantitative geomorphology. Geol Soc Amer Bull 56:275–370

Hosseinzadeh SR (2011) Drainage network analysis, comparis of Digital Elevation Model (DEM) from ASTER with high resolution satellite image and areal photographs. International Journal of Environmental Science and Development 2(3):194. https://doi.org/10.7763/IJESD.2011.V2.123

Jacques PD, Salvador ED, Rô M, Grohmann CH, Nummer AR (2014) Application of morphometry in neotectonic studies at the eastern edge of the Paraná Basin, Santa Catarina State, Brazil. Geomorphology 213:13–23. https://doi.org/10.1016/j.geomorph.2013.12.037

Jain SK, Singh RD, Seth SM (2000) Design flood estimation using GIS supported GIUH approach. Water Resour Manag 14:369–376. https://doi.org/10.1023/A:1011147623014

Javed A, Khanday MY, Ahmed R (2009) Prioritization of sub-watersheds based on morphometric and land use analysis using Remote Sensing and GIS techniques. J Indian Soc Remote Sens 37:261–274. https://doi.org/10.1007/s12524-009-0016-8

Jenson SK, Domingue JO (1988) Extracting topographic structure from digital elevation data for geographic information system analysis. Photogramm Eng Remote Sens 54(11):1593–1600

Jothimani M, Dawit Z, Mulualem W (2020) Flood Susceptibility modeling of Megech River Catchment, Lake Tana Basin, North Western Ethiopia, using morphometric analysis. Earth Syst Environ. https://doi.org/10.1007/s41748-020-00173-7

Kaplan ED, Hegarty CJ (2006) Understanding GPS: principles and applications. Artech House :379–380

Kannan R, Venkateswaran S, Vijay Prabhu M, Sankar K (2018) Drainage morphometric analysis of the Nagavathi watershed, Cauvery river basin in Dharmapuri district, Tamil Nadu, India using SRTM data and GIS. Data Br 19:2420–2426. https://doi.org/10.1016/j.dib.2018.07.016

Kasi V, Yeditha PK, Rathinasamy M, Pinninti R, Landa SR, Sangamreddi C, Agarwal A, Radha PRD (2020) A novel method to improve vertical accuracy of CARTOSAT DEM using machine learning models. Earth Sci Inf. https://doi.org/10.1007/s12145-020-00494-1

Korup O (2005) Geomorphic imprint of landslides on alpine river systems, southwest New Zealand. Earth Surf Process Landf 30:783–800. https://doi.org/10.1002/esp.1171

Lindsay JB, Evans MG (2008) The influence of elevation error on the morphometrics of channel networks extracted from DEMs and the implications for hydrological modelling. Hydrol Process 22:1588–1603. https://doi.org/10.1002/hyp.6728

Luo W, Harlin JM (2003) A theoretical travel time based on watershed hypsometry. J Am Water Resour Assoc 39:785–792. https://doi.org/10.1111/j.1752-1688.2003.tb04405.x

Maheswaran R, Khosa R, Gosain AK, Lahari S, Sinha SK, Chahar BR, Dhanya CT (2016) Regional scale groundwater modelling study for Ganga River basin. J Hydrol 541:727–741. https://doi.org/10.1016/j.jhydrol.2016.07.029

Masoud MH (2016) Geoinformatics application for assessing the morphometric characteristics' effect on hydrological response at watershed (casestudy of Wadi Qanunah, Saudi Arabia). Arab J Geosci 9:1–22. https://doi.org/10.1007/s12517-015-2300-y

Melton MA (1957) An analysis of the relations among elements of climate, surface properties, and geomorphology, Dept. Geol. Columbia Univ. Tech. Rep. 11, Proj. NR 389–042, Off. of Nav. Res., New York

Mesa LM (2006) Morphometric analysis of a subtropical Andean basin (Tucumán, Argentina). Environ Geol 50:1235–1242. https://doi.org/10.1007/s00254-006-0297-y

Miller VC (1953) Quantitative geomorphic study of drainage basin characteristics in the Clinch Mountain area, Virginia and Tennessee. Technical report (Columbia University. Department of Geology); no. 3

Morisawa ME (1962) Quantitative geomorphology of some watersheds in the Appalachian Plateau. Geol Soc Am Bull 73(9):1025–1046

Mueller JE (1968) An introduction to the hydraulic and topographic sinuosity indexes. Ann Assoc Am Geogr 58(2):371–385

Mukherjee S, Joshi PK, Mukherjee S, Ghosh A, Garg RD, Mukhopadhyay A (2013) Evaluation of vertical accuracy of open source Digital Elevation Model (DEM). Int J Appl Earth Obs Geoinf 21:205–217. https://doi.org/10.1016/j.jag.2012.09.004

Nag SK (1998) Morphometric analysis using remote sensing techniques in the Chaka sub-basin. J Indian Soc Remote Sens 26:70–76

Nitheshnirmal S, Thilagaraj P, Rahaman SA, Jegankumar R (2019) Erosion risk assessment through morphometric indices for prioritisation of Arjuna watershed using ALOS-PALSAR DEM. Model Earth Syst Environ 5:907–924. https://doi.org/10.1007/s40808-019-00578-y

Niyazi B, Zaidi S, Masoud M (2019) Comparative study of different types of digital elevation models on the basis of drainage morphometric parameters (case study of Wadi Fatimah Basin, KSA). Earth Syst Environ 3:539–550. https://doi.org/10.1007/s41748-019-00111-2

NRSA (National Remote Sensing Agency), (2007) Natural resources census: national land use and land cover mapping using multi-temporal AWiFS data, project report. Publication No. NRSA/LULC/1:250 K/2007-1National Remote Sensing Agency, Hyderabad, India

Obi Reddy GP, Maji AK, Gajbhiye KS (2004) Drainage morphometry and its influence on landform characteristics in a basaltic terrain, Central India - a remote sensing and GIS approach. Int J Appl Earth Obs Geoinf 6:1–16. https://doi.org/10.1016/j.jag.2004.06.003

Olszevski N, Filho EIF, da Costa LM, Schaefer CEGR, Souza ED, Costa ODAV (2011) Morphology and hydrological aspects of black river basin, division of state of Rio de Janeiro and Minas Gerais, Morfologia e aspectos hidrológicos da bacia hidrográfica do Rio Preto, divisa dos estados do Rio de Janeiro e de Minas Gerais. Rev Arvore 35:485–492. https://doi.org/10.1590/S0100-67622011000300011

Ozdemir H, Bird D (2009) Evaluation of morphometric parameters of drainage networks derived from topographic maps and DEM in point of floods. Environ Geol 56:1405–1415. https://doi.org/10.1007/s00254-008-1235-y

Pankaj A, Kumar P (2009) GIS-based morphometric analysis of five major sub-watersheds of Song River, Dehradun district, Uttarakhand with special reference to landslide incidences. J Indian Soc Remote Sens 37:157–166. https://doi.org/10.1007/s12524-009-0007-9

Patel A, Katiyar SK, Prasad V (2016) Performances evaluation of different open source DEM using differential global positioning system (DGPS). Egypt J Remote Sens Sp Sci 19:7–16. https://doi.org/10.1016/j.ejrs.2015.12.004

Prabhakaran A, Jawahar Raj N (2018) Mapping and analysis of tectonic lineaments of Pachamalai hills, Tamil Nadu, India using geospatial technology. Geol Ecol Landscapes 2:81–103. https://doi.org/10.1080/24749508.2018.1452481

Prabhakar AK, Singh KK, Lohani AK, Chandniha SK (2019) Study of Champua watershed for management of resources by using morphometric analysis and satellite imagery. Appl Water Sci 9:1–16. https://doi.org/10.1007/s13201-019-1003-z

Prakash K, Rawat D, Singh S, Chaubey K, Kanhaiya S, Mohanty T (2019) Morphometric analysis using SRTM and GIS in synergy with depiction: a case study of the Karmanasa River basin, North central India. Appl Water Sci 9:1–10. https://doi.org/10.1007/s13201-018-0887-3

Rahmati O, Samadi M, Shahabi H, Azareh A, Rafiei-Sardooi AH, Melesse AM, Pradhan B, Chapi K, Shirzadi A (2019) SWPT: an automated GIS-based tool for prioritization of sub-watersheds based on morphometric and topo-hydrological factors. Geosci Front 10:2167–2175. https://doi.org/10.1016/j.gsf.2019.03.009

Rai P K, Mishra V M, Mohan K (2017) A study of morphometric evaluation of the Son basin, India using geospatial approach. Remote Sensing Applications: Society and Environment 7:9–20

Rai PK, Mohan K, Mishra S, Ahmad A, Mishra VN (2017) A GIS-based approach in drainage morphometric analysis of Kanhar River Basin, India. Appl Water Sci 7:217–232. https://doi.org/10.1007/s13201-014-0238-y

Rather MA, Satish Kumar J, Farooq M, Rashid H (2017) Assessing the influence of watershed characteristics on soil erosion susceptibility of Jhelum basin in Kashmir Himalayas. Arab J Geosci 10:1–25. https://doi.org/10.1007/s12517-017-2847-x

Rawat KS, Singh SK, Singh MI, Garg BL (2019) Comparative evaluation of vertical accuracy of elevated points with ground control points from ASTERDEM and SRTMDEM with respect to CARTOSAT-1DEM. Remote Sens Appl Soc Environ 13:289–297. https://doi.org/10.1016/j.rsase.2018.11.005

Ray RK, Syed TH, Saha D, Sarkar BC (2020) Modeling the impact of rainfall variations and management interventions on the groundwater regime of a hard-rock terrain in central India. Hydrogeol J 28:1209–1227. https://doi.org/10.1007/s10040-020-02132-y

Sachindra DA, Ahmed K, Rashid MM, Shahid S, Perera BJC (2018) Statistical downscaling of precipitation using machine learning techniques. Atmos Res 212:240–258. https://doi.org/10.1016/j.atmosres.2018.05.022

Sangireddy H, Stark CP, Kladzyk A, Passalacqua P (2016) GeoNet: an open source software for the automatic and objective extraction of channel heads, channel network, and channel morphology from high resolution topography data. Environ Model Softw 83:58–73. https://doi.org/10.1016/j.envsoft.2016.04.026

Sarkar S, Gundekar HG (2007) Geomorphological parameters: are they indicators for installation of a hydropower site?. In International Conference on Small Hydropower-Hydro Sri Lanka (Vol. 22, p. 24)

Sarkar T, Kannaujiya S, Taloor AK, Ray PKC, Chauhan P (2020) Integrated study of GRACE data derived interannual groundwater storage variability over water stressed Indian regions. Groundw Sustain Dev 10:100376. https://doi.org/10.1016/j.gsd.2020.100376

Satheeshkumar S, Venkateswaran S (2018) Predilection of sustainable recharge structures using morphometric parameters and decision making model in the Vaniyar sub basin, South India. Appl Water Sci 8:1–18. https://doi.org/10.1007/s13201-018-0844-1

ScHUMM S (1954) Evolution of drainage systems and slopes in badlands at Perth Amboy, New Jersey: Dept. Geology, Columbia Univ (No. 8, pp. 271-30). New York, Tech Rept

Schumm SA (1956) Evolution of drainage systems and slopes in badlands at Perth Amboy, New Jersey. Bull Geol Soc Am 67(5):597–646

Setti S, Maheswaran R, Radha D, Sridhar V, Barik KK, Narasimham ML (2020) Attribution of hydrologic changes in a tropical river basin to rainfall variability and land-use change: case study from India. J Hydrol Eng 25:1–15. https://doi.org/10.1061/(ASCE)HE.1943-5584.0001937

Shortridge A, Messina J (2011) Spatial structure and landscape associations of SRTM error. Remote Sens Environ 115:1576–1587. https://doi.org/10.1016/j.rse.2011.02.017

Smith KG (1950) Standards for grading texture of erosional topography. Am J Sci 248:655–668

Strahler AN (1952) Dynamic basis of geomorphology. Geol Soc Am Bull 63(9):923–938

Strahler AN (1954) Statistical analysis in geomorphic research. J Geol 62(1):1–25

Strahler AN (1956) Quantitative slope analysis. Geol Soc Am Bull 67(5):571–596

Strahler AN (1957) Quantitative Analysis of watershed geomorphology, transactions of the American Geophysical Union. Trans Am Geophys Union 38:913–920

Strahler AN (1958) Dimensional analysis applied to fluvially eroded landforms. Geol Soc Am Bull 69(3):279–300

Strahler AN (1964) Part II. Quantitative geomorphology of drainage basins and channel networks. Handbook of Applied Hydrology. McGraw-Hill, New York, pp 4–39

Suwandana E, Kawamura K, Sakuno Y, Kustivanto E, Raharjo B (2012) Evaluation of aster GDEM2 in comparison with GDEM1, SRTM DEM and topographic-map-derived DEM using inundation area analysis and RTK-DGPS data. Remote Sens 4:2419–2431. https://doi.org/10.3390/rs4082419

Tachikawa T, Hato M, Kaku M, Iwasaki A (2011) Characteristics of ASTER GDEM version 2. In: 2011 IEEE International Geoscience and Remote Sensing Symposium. IEEE, pp 3657–3660

Tadono T, Ishida H, Oda F, Naito S, Minakawa K, Iwamoto H (2014) Precise global DEM generation by ALOS PRISM. ISPRS Ann Photogramm Remote Sens Spat Inf Sci II–4:71–76. https://doi.org/10.5194/isprsannals-II-4-71-2014

Thomas J, Joseph S, Thrivikramji KP, Abe G, Kannam N (2012) Morphometrical analysis of two tropical mountain river basins of contrasting environmental settings, the southern Western Ghats, India. Environ Earth Sci 66:2353–2366. https://doi.org/10.1007/s12665-011-1457-2

Vaze J, Teng J, Spencer G (2010) Impact of DEM accuracy and resolution on topographic indices. Environ Model Softw 25:1086–1098. https://doi.org/10.1016/j.envsoft.2010.03.014

Weydahl DJ, Sagstuen J, Dick B, Rønning H (2007) SRTM DEM accuracy assessment over vegetated areas in Norway. Int J Remote Sens 28:3513–3527. https://doi.org/10.1080/01431160600993447

Yue L, Shen H, Zhang L, Zheng X, Zhang F, Yuan Q (2017) High-quality seamless DEM generation blending SRTM-1, ASTER GDEM v2 and ICESat/GLAS observations. ISPRS J Photogramm Remote Sens 123:20–34. https://doi.org/10.1016/j.isprsjprs.2016.11.002

Zheng X, Xiong H, Gong J, Yue L (2015) A robust channel network extraction method combining discrete curve evolution and the skeleton construction technique. Adv Water Resour 83:17–27. https://doi.org/10.1016/j.advwatres.2015.05.003